IDENTFICATION OF MAIN FACTORS OF UNCERTAINTY IN A MICROSTRIP LINE NETWORK

Progress In Electromagnetics Research, Vol. 162, 61–72, 2018

Identification of Main Factors of Uncertainty in a Microstrip Line Network

Mourad Larbi[1, *], Igor S. Stievano[1], Flavio G. Canavero[1], and Philippe Besnier[2]

Abstract—This paper deals with uncertainty propagation applied to the analysis of crosstalk in printed circuit board microstrip traces. Complex interconnection networks generally are affected by many uncertain parameters and their point-to-point transfer functions are computationally expensive, thus making Monte-Carlo analyses rather inefficient. To overcome this situation, a metamodel is highly desirable. This paper presents a sparse and accelerated polynomial chaos approach, which proves to be well adapted for high-dimensional uncertainty quantification and well suited for the sensitivity analysis of crosstalk effects. We highlight the significant advantage of the advocated approach for the design of microstrip line networks of complex topology. In fact, we demonstrate how a small number of system simulations can help to quantify the statistics of the output variability and identify a reduced set of high-impact parameters.

1. INTRODUCTION

In modern electronic circuits, the density of packages and interconnections is so high that the analysis of signal propagation and power distribution in printed circuit boards is challenging in terms of computer resources and simulation time. Additional crucial requirements are introduced if we intend to assess the impact of tolerances or parameters variability on the system performance, since we need to run a large number of deterministic simulations either to optimize the design or to determine the risk of non-compliance with specifications. Parameters uncertainties arise from temperature variations, intrinsic characteristics of materials, geometrical and electrical tolerances, etc., that may generate a large variability of output signals.

To address the problem of uncertainty quantification (UQ) of high-speed information and communication systems, several approaches based on the so-called polynomial chaos (PC) technique have been successfully developed [1–3]. This technique represents the random response of a model in terms of a linear combination of orthonormal polynomial basis involving the input random variables. Intrusive [3–5] or non-intrusive [2, 6, 7] approaches exist for the computation of the basis coefficients, thus reproducing an analytic representation called metamodel (or surrogate model) of the system response. The metamodel can be profitably used to estimate statistical quantities of the system output, like moments and probability density functions (PDF). Although this technique has been satisfactorily employed in many examples, it suffers when the input dimensionality of the problem significantly increases, since the computational cost of the numerical model rapidly grows. To face this problem, referred to as the *curse of dimensionality*, few approaches have been lately introduced in the context of high-speed circuits [8, 9]. In the field of probabilistic engineering mechanics, another approach named the *sparse PC* and based on the *Least Angle Regression* (LARS) algorithm [10] has been successfully used in order to quantify uncertainties in high-dimensional problems. This paper proposes to evaluate

Received 6 April 2018, Accepted 13 May 2018, Scheduled 13 June 2018

* Corresponding author: Mourad Larbi (mourad.larbi@polito.it).

[1] Dipartimento di Elettronica e Telecomunicazioni, EMC Group, Politecnico di Torino, Torino 10129, Italy. [2] Institut d'Électronique et de Télécommunications de Rennes (IETR), UMR CNRS 6164, INSA de Rennes, Rennes 35043, France.

this method in order to deal with uncertainties in an electronic circuit [11]. First, the method is introduced in Section 2. The approach is then applied to the analysis of the crosstalk transfer function in Section 3. This application evaluates the variability of the model response in low and high frequency domain. Moreover, the impact of uncertain input parameters on the crosstalk response is quantified via a sensitivity analysis. We evidence that, despite an important number of uncertain parameters, only a few of them have a significant impact on the point-to-point transfer function under analysis. The metamodel provides a powerful tool to reduce the dimensionality of the initial problem.

2. POLYNOMIAL CHAOS EXPANSION

2.1. Introduction

Let $\mathbf{X}$ be a random vector of joint PDF $f_{\mathbf{X}}(\mathbf{x})$, including M random variables $(X_1, \ldots, X_M)$ assumed to be independent and representing the uncertain input parameters of the problem. Let $Y = \mathcal{M}(\mathbf{X})$ be the random scalar response of a numerical model $\mathcal{M}$ describing the physical system. Assuming that the random response Y has a finite variance, we can write [12]:

$$Y = \sum_{\boldsymbol{\lambda} \in \mathbb{N}^M} a_{\boldsymbol{\lambda}} \Phi_{\boldsymbol{\lambda}}(\mathbf{X}), \tag{1}$$

where a_λ are the unknown deterministic coefficients, and $\Phi_{\boldsymbol{\lambda}}$ represent a basis of multivariate polynomials, which are orthonormal with respect to the joint PDF $f_{\mathbf{X}}(\mathbf{x})$, i.e., $\mathbb{E}[\Phi_\lambda(\mathbf{X})\Phi_\beta(\mathbf{X})] = \delta_{\lambda\beta}$, with $\delta_{\lambda\beta} = 1$ if $\lambda = \beta$ and 0 otherwise. In practice, families of orthonormal polynomials are associated in terms of probability distributions of input random variables.

Let $\mathcal{X} = \{\mathbf{x}^{(1)}, \ldots, \mathbf{x}^{(n)}\}$ be a set of realizations of $\mathbf{X}$, denoted as an *experimental design* (ED), and $\mathcal{Y} = \{\mathcal{M}(\mathbf{x}^{(1)}), \ldots, \mathcal{M}(\mathbf{x}^{(n)})\}$ be the associated set of model response quantities. Using this set of model evaluations, the coefficients of the PC representation may be estimated by using non-intrusive techniques. Among these techniques, the ordinary least square regression [13] may be employed.

2.2. From Classical Truncation Scheme to Sparse Chaos Representation

In order to calculate the polynomial expansion, the infinite series in Eq. (1) has to be truncated. The usual truncation rule consists in choosing a maximum polynomial degree l, which means preserving all polynomials associated to the set $\mathcal{A}^{M,l} = \{\boldsymbol{\lambda} \in \mathbb{N}^M : \|\boldsymbol{\lambda}\|_1 = \sum_{i=1}^M \lambda_i \leq l\}$. Thus, the cardinal of the set $\mathcal{A}^{M,l}$ denoted $L = \dfrac{(M+l)!}{M!\, l!}$ increases quickly with the number of input random variables M and the degree l of the polynomials; For example, $M = 10$ and $l = 5$ lead to $L = 3003$. For M typically larger than 10, advanced truncation schemes are required.

An improved truncation scheme [10] based on a parameter k $(0 < k \leq 1)$ is given by:

$$\mathcal{A}^{M,l,k} = \left\{ \boldsymbol{\lambda} \in \mathbb{N}^M : \|\boldsymbol{\lambda}\|_k = \left(\sum_{i=1}^M \lambda_i^k \right)^{1/k} \leq l \right\}. \tag{2}$$

This hyperbolic truncation strategy favors the most relevant effects and low-order interactions, which mainly impact the response according to the *sparsity-of-effects principle* [14]. The lower is k, the more high-rank interactions will be discarded. Moreover, when $k = 1$, this scheme is equivalent to the classical PC approximation defined by the truncation set $\mathcal{A}^{M,l}$. When $k < 1$, the remaining terms of the polynomial basis can be significantly reduced compared to L [10]. This hyperbolic truncation scheme for two input random variables ($M = 2$) is illustrated in Figs. 1(a) and 1(b), where the circles represent all terms of the polynomial basis of degree less than or equal to $l = 5$, included in the set (2) for $k = 1$ (blue circles) and $k = 0.5$ (pink circles). From Fig. 1, it is evident that $k = 0.5$ selects a number of polynomials (pink circles) much smaller than those generated by the standard truncation set $\mathcal{A}^{M,l}$ (blue circles).

The hyperbolic truncation strategy is a first step towards a sparse PC expansion of the response, represented by a truncation set $\mathcal{A}^{M,l,k}$ of cardinal K, potentially much lower than L. However, the

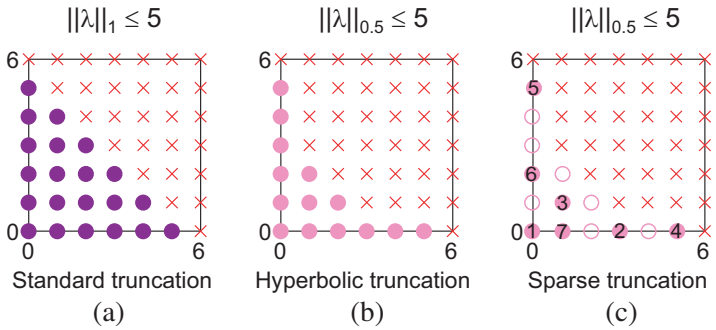

Figure 1. Polynomial basis terms of degree less than or equal to $l = 5$ retained by the hyperbolic truncation strategy when (a) $k = 1$ (blue circles) and (b) $k = 0.5$ (pink circles). (c) Numbered pink circles are the polynomial basis terms selected by the LARS algorithm at the ith iteration ($i = 1, \ldots, 7$) [10].

retained number of terms of the polynomial basis may be further reduced by using the LARS [15] selection algorithm.

A brief summary of LARS follows, whereas the reader is referred to [10] for additional details. LARS consists in an iterative process, producing a sparse representation containing from 1 to K terms of the polynomial basis (from one to all the pink circles in Fig. 1(b)), according to their decreasing impact. The algorithm begins by selecting the basis $\Phi_{\boldsymbol{\lambda}_1}$, which best correlates with the response Y. In practice, the correlation is computed from a set of random realizations of the response $\mathcal{Y}$. Once the first polynomial $\Phi_{\boldsymbol{\lambda}_1}$ is obtained, its weighting coefficient is estimated so that the residual $Y - a^{(1)}_{\boldsymbol{\lambda}_1}\Phi_{\boldsymbol{\lambda}_1}(\boldsymbol{X})$ becomes as much correlated with another basis, identified as $\Phi_{\boldsymbol{\lambda}_2}$. The first two elements so selected will help incorporate a third one by moving along the direction $(\Phi_{\boldsymbol{\lambda}_1} + \Phi_{\boldsymbol{\lambda}_2})$, until the new residual becomes equi-correlated with a third polynomial basis $\Phi_{\boldsymbol{\lambda}_3}$, and so on. An illustration of the outcome of the LARS algorithm is given in Fig. 1(c), where the retained bases after seven iterations are identified by pink circles.

The selection process of appropriate polynomials by LARS algorithm is carried out for each degree $l = 1, 2, \ldots, l_{\max}$. The quality of each metamodel of order l is computed from the following criterion error.

Let denote by $\mathcal{M}^{PC}_{-i}$ the metamodel built up from the ED $\mathcal{X} \setminus \mathbf{x}^{(i)}$, i.e., considering all realizations except the ith. The residual of this metamodel is then estimated by the difference between the model response at the realization $\mathbf{x}^{(i)}$ and its prediction given by the metamodel $\mathcal{M}^{PC}_{-i}$, i.e., $\delta^{(i)} = \mathcal{M}(\mathbf{x}^{(i)}) - \mathcal{M}^{PC}_{-i}(\mathbf{x}^{(i)})$. Finally, the leave-one-out error of the metamodel is estimated by:

$$\epsilon_{LOO} = \sum_{i=1}^{N} \left(\delta^{(i)}\right)^2. \tag{3}$$

The selected degree l (and its associated sparse polynomial basis) is the one minimizing the leave-one-out error ϵ_{LOO}.

In the following, the quality of the metamodel will be computed via the Q^2 coefficient defined by $Q^2 = 1 - \epsilon_{LOO}$, $0 \leq Q^2 \leq 1$. Note that the larger is Q^2, the better is the prediction of the generated metamodel.

2.3. Quantities of Interest Obtained by Post-processing

The generated PC expansion provides, at a negligible computational cost, statistical quantities of the response. In particular, the orthonormality property of the basis, allows us to obtain the expectation and the variance of the output Y as follows:

$$\mathbb{E}[Y] = a_{\mathbf{0}} \tag{4}$$

$$\mathbb{V}[Y] = \sum_{\lambda \in \mathcal{A} \setminus \{\mathbf{0}\}} a_\lambda^2 \tag{5}$$

In addition, sensitivity analysis can be obtained by means of *Sobol indices* [16], in order to quantify the impact of uncertain input variables on the response Y. Thus, the *PC-based Sobol indices* of *first-order* S_i and the *total indices* $S_{T,i}$ of the response Y with respect to the input random variable X_i are computed, according to [17]:

$$S_i = \frac{\sum_{\lambda \in \mathcal{A}_i} a_\lambda^2}{\mathbb{V}[Y]} \tag{6}$$

where $\mathcal{A}_i = \{\lambda \in \mathcal{A} : \lambda_i > 0, \lambda_j = 0 \; \forall j \neq i\}$, and

$$S_{T,i} = \frac{\sum_{\lambda \in \mathcal{A}_{T,i}} a_\lambda^2}{\mathbb{V}[Y]} \tag{7}$$

where $\mathcal{A}_{T,i} = \{\lambda \in \mathcal{A} : \lambda_i \neq 0\}$, respectively.

3. UNCERTAINTY QUANTIFICATION OF THE CROSSTALK EFFECT IN A TRANSMISSION LINE NETWORK

3.1. Presentation of the Crosstalk Configuration

This section considers the lossless transmission line network represented in Fig. 2. This test case is inspired from [18], but the size has been increased. The voltage source V_1 of the network is a sine wave sweeping the frequency band [100 MHz–3 GHz]. The pieces of coupled microstrip lines have a nominal length of 3 cm. The variability of the network is introduced via all lumped elements and all cross section parameters. Note that the copper trace width w_i, trace thickness t_i, trace-to-trace separation d_i are related to each piece of line $\#i$, while the substrate dielectric relative permittivity ϵ_r and the substrate thickness h are associated to all lines. This example deals with 48 uncertain parameters, which are considered as uniform random variables having an uncertainty of 20% around their nominal values given in Fig. 2.

The impact of these uncertain parameters will be analyzed on the transfer function magnitude $|H_1| = 20 \times \log|\frac{V_{out}}{V_1}|$ dB, defined as the ratio between the far-end crosstalk voltage magnitude and the

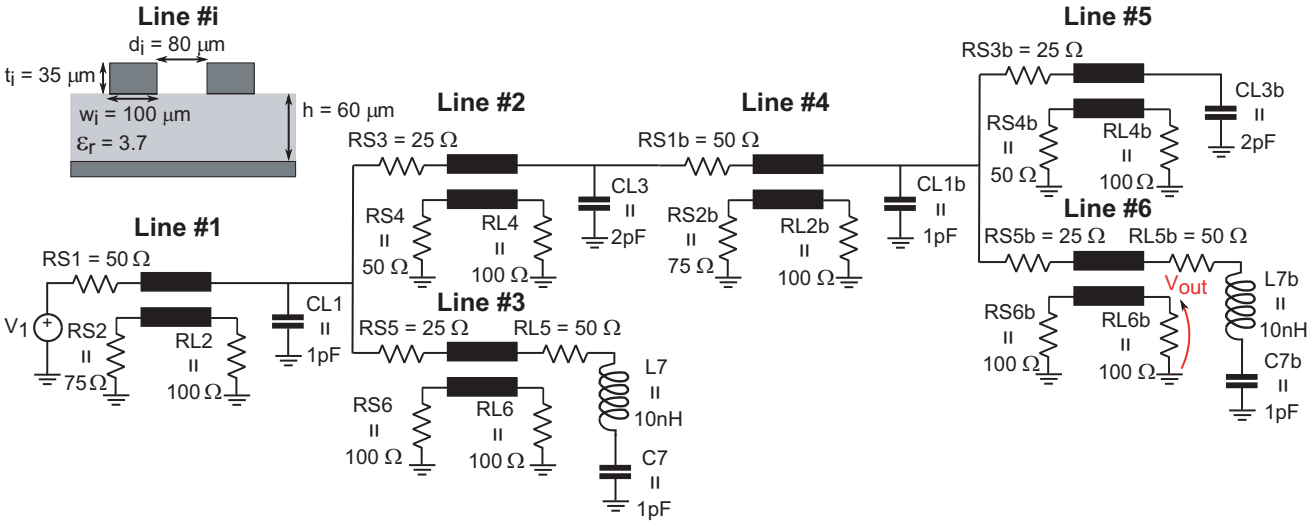

Figure 2. Transmission line network with coupled microstrip traces and corresponding line cross section.

source excitation magnitude. The reference evaluation of $|H_1|$ in the frequency domain, denoted by $\mathcal{M}$ in the following, is numerically calculated via a MATLAB implementation of the standard modified nodal analysis (MNA).

The goal of the study is to build up a sparse PC metamodel of $|H_1|$ over the frequency band [100 MHz–3 GHz] in order to reduce the computational cost of the numerical model $\mathcal{M}$. Further, we would like to quantify the impact of uncertain parameters on the variability of $|H_1|$.

3.2. Numerical Results and Discussion

The results presented in this section are obtained from the UQLAB toolbox (Uncertainty Quantification toolbox in MATLAB) [19].

3.2.1. Sparse PC Metamodel

This section aims at analyzing the impact of uncertain input parameters on the transfer function $|H_1|$ in the frequency band [100 MHz–3 GHz]. For this, a sparse PC approximation is built up via 200 realizations from Latin Hypercube Sampling (LHS) [20] and an adaptive degree l comprised between 1 and 5. The latter choice is motivated by the behavior of $|H_1|$, which is smooth at low frequency and irregular at higher frequencies. Since the number of input variables is large (i.e., 48), the size of the polynomial basis is reduced by means of the hyperbolic truncation scheme (2), for which we have chosen $k = 0.6$. Note that no rigorous method is available on how to choose it, only empirical guidelines are known [10].

After having carried out a sparse PC approximation for 301 logarithmically spaced frequencies, we are interested in evaluating the quality of the metamodel. Fig. 3(a) represents the Q^2 coefficient over the entire frequency band [100 MHz–3 GHz]. We observe that the Q^2 coefficient ranges between 0.95 and 1 in the [100 MHz–1.5 GHz] frequency band, and is reduced between 0.87 and 0.97 in the [1.5 GHz–3 GHz] frequency interval. Consequently, the quality level of the sparse PC approximation is very good in the frequency band [100 MHz–1.5 GHz], but the technique may be less efficient over the frequency band

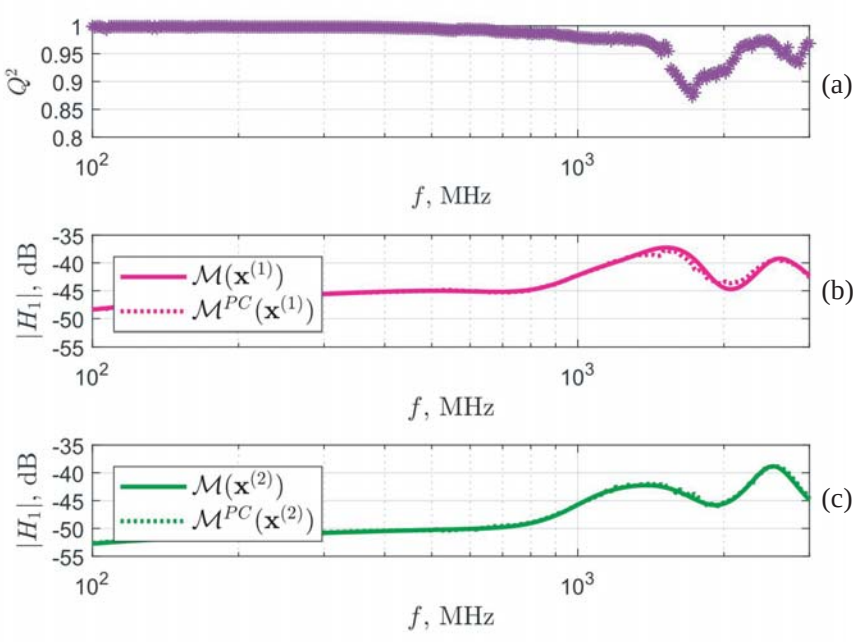

Figure 3. (a) Behavior of the Q^2 coefficient of the sparse PC metamodel over the frequency band [100 MHz–3 GHz]. (b) and (c) Calculation of the transfer function $|H_1|$ by the sparse PC metamodel $\mathcal{M}^{PC}$ (dotted-line) and by the numerical model $\mathcal{M}$ (solid line) from two MC realizations.

[1.5 GHz–3 GHz]. This is clearly correlated with the variability of the transfer function $|H_1|$ which is stronger in the resonance area. We thus illustrate in Figs. 3(b) and (c), the evolution of $|H_1|$ computed by the sparse PC metamodel $\mathcal{M}^{PC}(\mathbf{x}^{(i)})$ (dotted-line) and by the numerical model $\mathcal{M}(\mathbf{x}^{(i)})$ (solid line) from two Monte Carlo (MC) realizations: the result is, that the sparse PC fits very well the evolution of $|H_1|$ over the entire frequency band [100 MHz–3 GHz], in spite of small differences around the resonance peaks, between 1 GHz and 3 GHz.

We intend now to discuss the efficiency of the sparse PC at two different frequencies: we have chosen 202 MHz as a representative example of the smooth behavior of $|H_1|$, where $Q^2_{202\,\mathrm{MHz}} = 99.80\%$, and 2.23 GHz as an illustrative example of the irregular behavior, where $Q^2_{2.23\,\mathrm{GHz}} = 96.62\%$. Fig. 4 shows the PDF of $|H_1|$ computed from 10000 MC realizations; the dashed line represents the result of the sparse PC metamodel and the solid line refers to the reference model MC simulations, for the frequencies of 202 MHz and of 2.23 GHz. At 202 MHz, we observe a perfect agreement between the blue and red curves, meaning a high level of accuracy of the sparse PC metamodel. For instance, the expectation and the standard deviation of the response $|H_1|$ given by sparse PC metamodel and by MC simulation are very close, i.e., $\mu^{PC} = -46.51$ dB, $\sigma^{PC} = 2.36$ dB and $\mu^{MC} = -46.52$ dB, $\sigma^{MC} = 2.37$ dB, respectively.

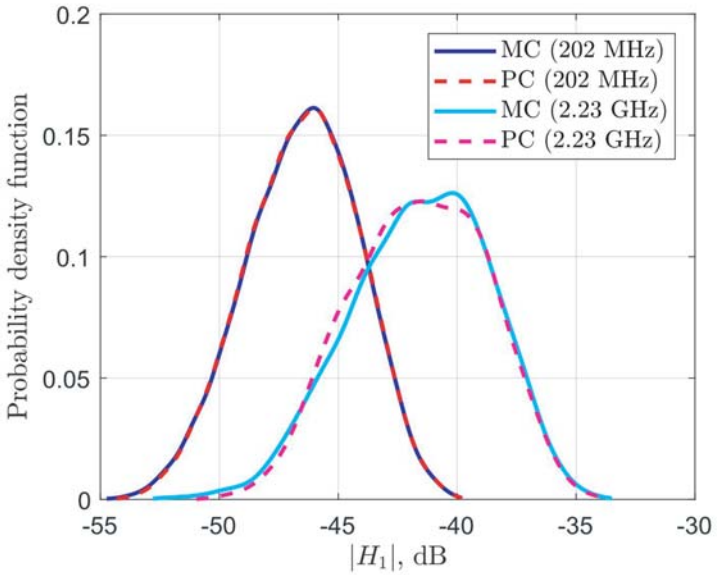

Figure 4. PDF of the transfer function $|H_1|$ obtained by sparse PC (dashed-lines) and by MC simulation (solid lines) at the frequencies of 202 MHz and of 2.23 GHz.

For the frequency of 2.23 GHz, Fig. 4 shows that the sparse PC (magenta dashed-line) fits reasonably well with the PDF estimated from MC simulation (cyan solid line), even though small discrepancies appear at the level of the main tendency and of the tails of the probability distribution. In such a case, there is a small difference between the estimation of the expectation and the standard deviation obtained by sparse PC and MC simulation: $\mu^{PC} = -41.60$ dB, $\sigma^{PC} = 2.82$ dB and $\mu^{MC} = -41.58$ dB, $\sigma^{MC} = 2.93$ dB, respectively.

It is worth adding some comments to the above analysis of the sparse PC results for the two frequencies. Even if, for both frequencies, the optimal degree needed by the sparse PC is 4, and 49 polynomial bases were required out of the 1321 elements of the full basis (corresponding to a sparsity index $SI = \frac{49}{1321} = 3.71\%$), we notice that the method is less efficient for the higher frequency. This may be explained in part by the variability of the transfer function $|H_1|$, which is higher in the resonance region. As regards the computational time used for the calculation of $|H_1|$ over the frequency band [100 MHz–3 GHz], the sparse PC required 3.30 s whereas 10000 MC realizations took 2 h 50 min, with a speed up of about 3096× for the sparse PC metamodel over the MC simulation. Note that this

computational cost does not take into account the training time which has taken about 12 min, whose 9 min are required by the LARS algorithm and 3 min are needed for the 200 LHS simulations.

3.2.2. Sensitivity Analysis

In addition to the estimation of the variability of $|H_1|$, the sparse PC metamodel allows for a sensitivity analysis of the response (see Section 2.3). In Fig. 5, a histogram presents the maximum values of the total Sobol indices of $|H_1|$, obtained according to (7), in the frequency band [100 MHz–3 GHz]. From Fig. 5, it is evident that 23 random variables out of the 48 initial input variables have a non negligible contribution, defined as the maximum of total Sobol indices higher than or equal to 2% (red dashed line), on the variability of $|H_1|$. The variables having the largest impact on the variations of the response $|H_1|$ in the entire frequency band are the following parameters: the relative permittivity ϵ_r and the thickness h of the substrate, along with the trace-to-trace separation d_6 of the coupled line #6. Besides, we remark that several lumped elements, among which $C7b$, $L7b$, $CL3$, $RS1$, $RL6b$, $RS1b$, have the largest influence. Lastly, the trace widths w_6, w_2 and w_5 of lines #6, #2 and #5, respectively, have less effect on the variability of response $|H_1|$.

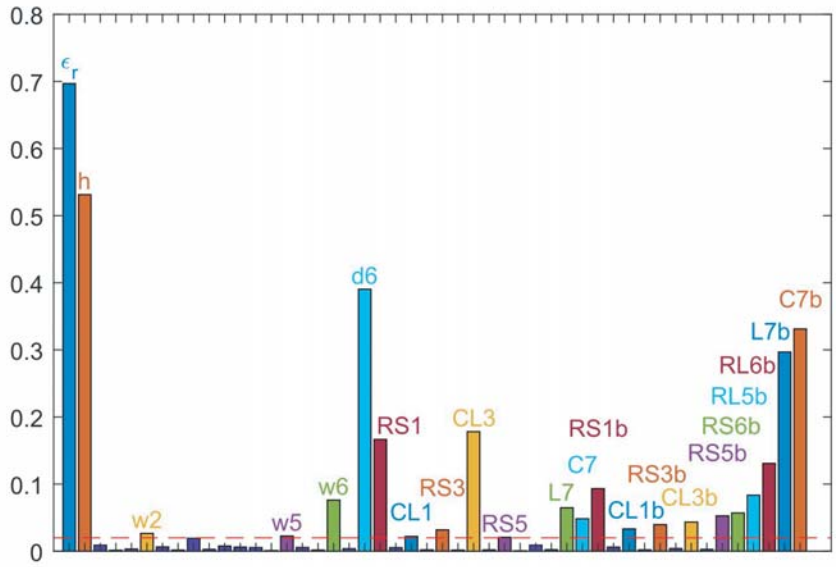

Figure 5. Maximum values, over the frequency band [100 MHz–3 GHz], of total Sobol indices of the transfer function $|H_1|$. The red dashed-line represents the selected 2% threshold for the impact of uncertain input parameters.

To quantify more accurately the impact of the 23 input variables depicted in Fig. 5, we show in Fig. 6 the total Sobol indices of these parameters in the frequency band [100 MHz–3 GHz]. Looking at Fig. 6, we observe that, from 100 MHz to around 1 GHz, the variability of $|H_1|$ is mainly associated with the substrate thickness h, the trace-to-trace separation d_6 of the coupled line #6 and, to a lesser extent, various components as, e.g., $RS1$, $RS3$, $RS1b$, $RS6b$, $RL6b$ etc.. Next we observe that, from 1 GHz to 3 GHz, the variations of $|H_1|$ are sensitive to a larger number of uncertain variables such as the substrate relative permittivity ϵ_r (with the largest impact between 2 GHz and 2.5 GHz), the substrate thickness h, and the terminal components $L7b$ and $C7b$ of the network. Other variables, such as the trace width w_6 and the trace-to-trace separation d_6 of line #6, and some lumped elements as, e.g., $RS1$, $CL3$, $L7$, $C7$, $RS1b$, have a smaller effect on the variability of the response $|H_1|$. It is worth mentioning that the sensitivity analysis presents a larger number of components in the resonance region.

From the physical point of view, the hierarchy of the input uncertainties is coherent. Indeed, we retrieve an important impact of the trace-to-trace separation d_6 and the components $L7b$ and $C7b$,

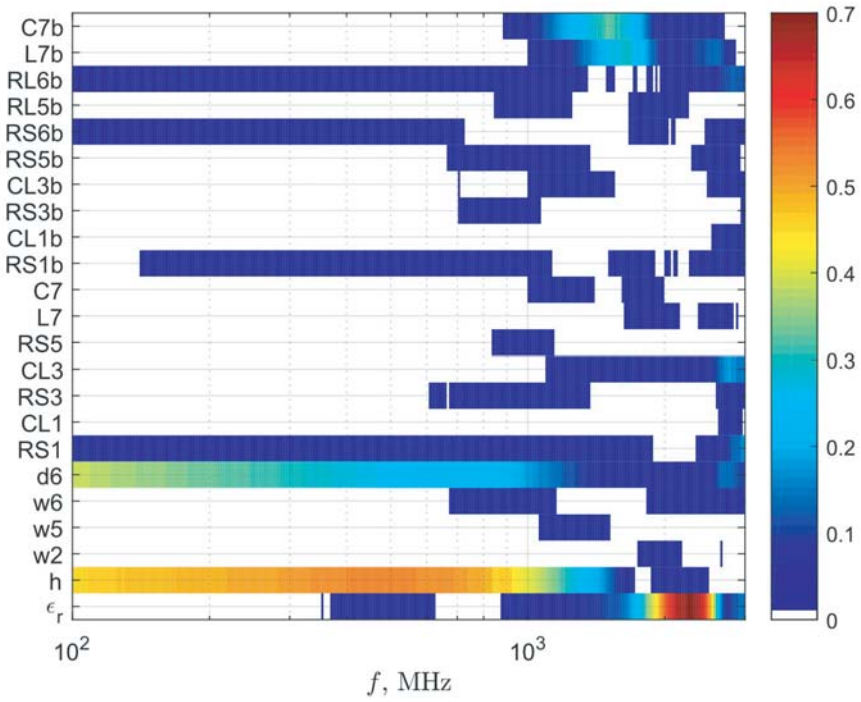

Figure 6. Total Sobol indices of the transfer function $|H_1|$ over the frequency band [100 MHz–3 GHz].

which are the variables related to the coupled line #6, where the crosstalk transfer function $|H_1|$ is computed. Moreover, the observation of a very large contribution of the dielectric relative permittivity ϵ_r of the substrate is also consistent, since dielectric properties strongly impact the position in frequency of the resonance peak of the coupled line of fixed length.

3.2.3. Reduction of the Number of Uncertain Variables

As mentioned above, the sensitivity analysis given in Fig. 5 shows that, among the 48 input random variables, 25 variables have a minimal impact over the entire frequency band [100 MHz–3 GHz], where their total Sobol indices are always less than 2%. Since these variables have a negligible effect on the variability of the response $|H_1|$, we decided to set them to their nominal values given in Fig. 2. We illustrate now the behavior of $|H_1|$ evaluated by the model $\mathcal{M}$ on the remaining 23 impacting variables. In Fig. 7, we represent the evolution of the response $|H_1|$ in the frequency band [100 MHz–3 GHz] calculated by the numerical model $\mathcal{M}$ from three MC realizations of the complete set $\mathbf{x}^{(i)}$ of 48 random variables and of the reduced set $\tilde{\mathbf{x}}^{(i)}$ of 23 random variables (i.e., same realizations for the complete and reduced sets of random variables, and nominal values for the other 25 variables of this latter). Fig. 7 shows a very good agreement between $|H_1|$ evaluated by $\mathcal{M}(\mathbf{x}^{(i)})$ (solid line) and by $\mathcal{M}(\tilde{\mathbf{x}}^{(i)})$ (squares). This confirms that the 25 random variables, fixed at their nominal value, do not produce a significant contribution to the variations of the response $|H_1|$. Therefore, the number of uncertain variables can be reduced by about 50% without degrading the variations of $|H_1|$ over the frequency band [100 MHz–3 GHz].

3.2.4. Analysis of Extreme Values

As discussed in Section 3.2.1, the sparse PC metamodel has a very good quality over almost all the frequency band [100 MHz–3 GHz]. For instance, from Fig. 4, we observe that the PDFs of the response $|H_1|$ computed by the sparse PC metamodel and by MC simulation (adopted as the reference) are in excellent agreement at 202 MHz, and reasonably compare at 2.23 GHz. Observing the curves of Fig. 4,

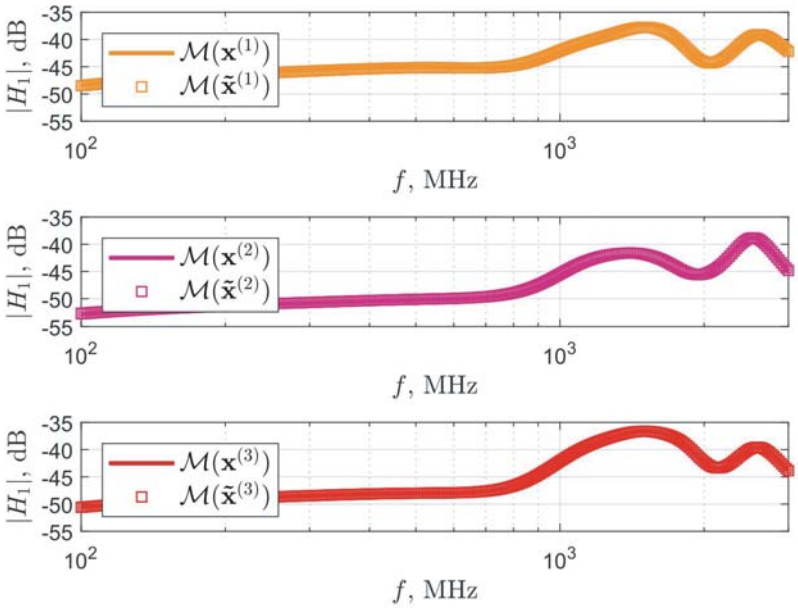

Figure 7. Illustration of the transfer magnitude function $|H_1|$ over the frequency band [100 MHz–3 GHz]. The transfer function $|H_1|$ is computed from the numerical model $\mathcal{M}$, evaluated for three different sets of input random parameters: solid lines reproduce the results of the full set $\mathbf{x}^{(i)}$ of 48 random variables; squares refer to the use of the reduced set $\tilde{\mathbf{x}}^{(i)}$ of 23 random variables.

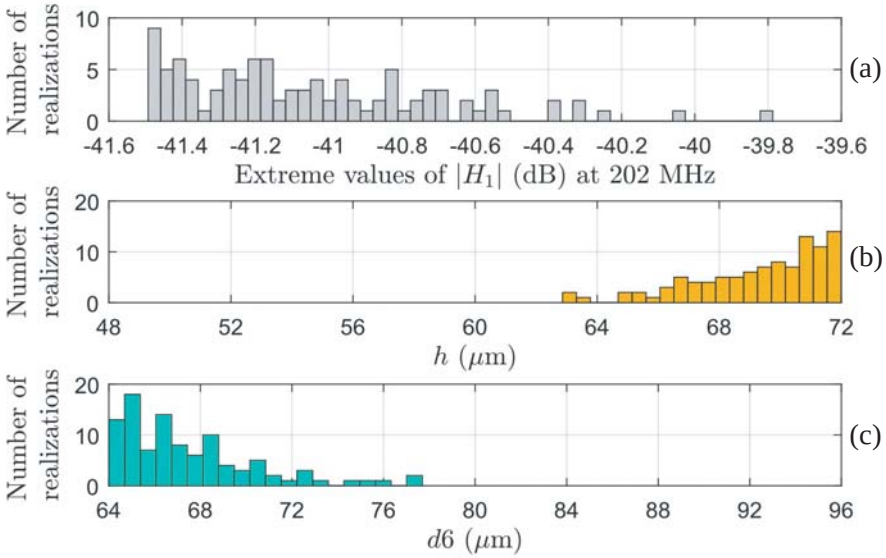

Figure 8. Extreme crosstalk levels of $|H_1|$ (a) obtained by the sparse PC metamodel, at 202 MHz. The distributions of values of the substrate thickness h and of the trace-to-trace separation d_6 of the coupled line #6 contributing to (a) the top histogram are represented in (b) and (c), respectively.

we notice that the sparse PC metamodel produces a very good fitting at the level of the right tails of the PDFs of $|H_1|$, related to the largest extreme values. Thus, from the sparse PC metamodel, we propose to identify extreme values of $|H_1|$, e.g., larger than the 99% quantile. The histogram of Fig. 8(a) represents the extreme values (highest 0.99-quantile) of $|H_1|$, at 202 MHz. The extreme values range from -41.5 dB to -39.8 dB. Since extreme values are very important from the design point of view, it

might be interesting to check if they are obtained for specific configurations of input parameters. In fact, the sensitivity analysis at 202 MHz given in Fig. 6 points out to the substrate thickness h and the trace-to-trace separation d_6 of the coupled line #6 as the most impacting parameters on the variability of $|H_1|$ (h accounts for approximately 50% of the total impact, while d_6 for about 30%). Figs. 8(b) and (c) represent histograms of the input realizations of the random variables h and d_6 producing the extreme values of $|H_1|$ at 202 MHz. We notice that the extreme levels of $|H_1|$ are obtained for large values of the substrate thickness h, i.e., between 62.9 µm and 72.0 µm (the nominal value being 60 µm), and small values of the trace-to-trace separation d_6 of the line #6, i.e., between 64.0 µm and 77.7 µm (the nominal value being 80 µm). This observation is physically consistent, since the crosstalk coupling is usually higher when the traces are closer (tighter coupling) and are far from the ground plane (field lines spread out and are more likely to interfere with an adjacent circuit). This analysis of extreme values seems therefore be in line with the sensitivity analysis outcomes depicted in Fig. 6.

The same analysis of extreme values of the transfer function $|H_1|$ carried out at 2.23 GHz reveals different properties of the propagation structure. The upper panel of Fig. 9 represents the extreme values (highest 0.99-quantile) of $|H_1|$, ranging from -35.9 dB to -33.9 dB. The sensitivity analysis of Fig. 6 highlights that, at 2.23 GHz, the dielectric relative permittivity ϵ_r is the predominant variable, with an impact on the order of 60% of the total variability of the response $|H_1|$. The lower panel of Fig. 9 represents the distribution of values of the dielectric relative permittivity ϵ_r contributing to extreme crosstalk levels of $|H_1|$. We notice that the extreme levels of $|H_1|$ are obtained for large values of the substrate relative permittivity, i.e., between 3.96 and 4.44 (the nominal value being 3.7). Once again, this particular input range of the dielectric relative permittivity ϵ_r seems to be in agreement with the sensitivity analysis outcomes of Fig. 6 at 2.23 GHz.

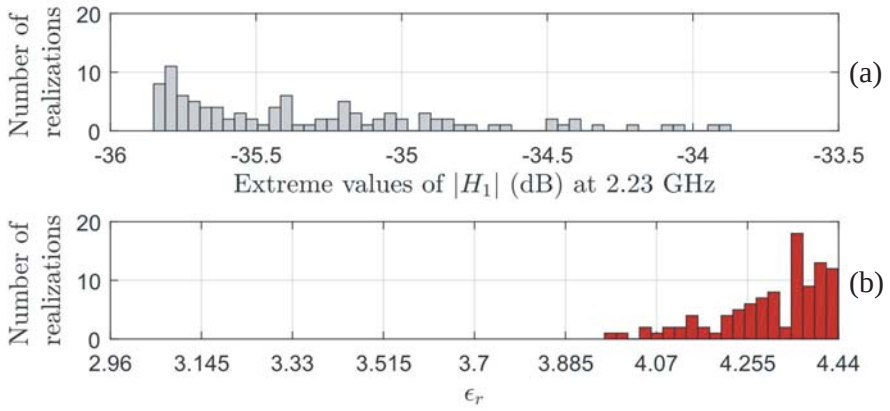

Figure 9. (a) Extreme crosstalk levels of $|H_1|$ obtained by the sparse PC metamodel, at 2.23 GHz. The distribution of values of the substrate relative permittivity ϵ_r contributing to (a) the top histogram is represented in (b).

4. CONCLUSION

This paper presents the application of the sparse PC metamodel to the design of a microstrip transmission line network with many uncertain parameters. The crosstalk response of the system is expanded on a multivariate polynomial basis of input random variables in order to reduce the computational cost compared to MC simulation. The efficiency of this PC representation consists in providing a very good approximation of the output by means of a small number of simulations, despite a large number of uncertain input parameters. The usefulness of this method resides in the estimation of statistical quantities such as the PDF of the system response. It may also provide a quantification of uncertain input parameters according to their influence on the variability of the output.

As illustrated above for the microstrip line network, the variability of the crosstalk response is mainly explained by a small group of input variables, which are the thickness and the relative

permittivity of the substrate, as well as the trace-to-trace separation of the coupled line on which the output is observed. This information, derived from the sparse PC metamodel, may be very useful in the design phase of a system since it points out to the sensitivity issues of the system response. For example, the identification of parameters causing important variations of the response can allow to anticipate potential failures of the system and to properly size margins for the design.

REFERENCES

1. Rong, A. and A. C. Cangellaris, "Interconnect transient simulation in the presence of layout and routing uncertainty," *2011 IEEE 20th Conference on Electrical Performance of Electronic Packaging and Systems*, 157–160, Oct. 2011.
2. Prasad, A. K., M. Ahadi, B. S. Thakur, and S. Roy, "Accurate polynomial chaos expansion for variability analysis using optimal design of experiments," *2015 IEEE MTT-S International Conference on Numerical Electromagnetic and Multiphysics Modeling and Optimization (NEMO)*, 1–4, Aug. 2015.
3. Ginste, D. V., D. D. Zutter, D. Deschrijver, T. Dhaene, P. Manfredi, and F. Canavero, "Stochastic modeling-based variability analysis of on-chip interconnects," *IEEE Transactions on Components, Packaging and Manufacturing Technology*, Vol. 2, No. 7, 1182–1192, Jul. 2012.
4. Biondi, A., P. Manfredi, D. V. Ginste, D. D. Zutter, and F. G. Canavero, "Variability analysis of interconnect structures including general nonlinear elements in spice-type framework," *Electronics Letters*, Vol. 50, No. 4, 263–265, Feb. 2014.
5. Pham, T. A., E. Gad, M. S. Nakhla, and R. Achar, "Decoupled polynomial chaos and its applications to statistical analysis of high-speed interconnects," *IEEE Transactions on Components, Packaging and Manufacturing Technology*, Vol. 4, No. 10, 1634–1647, Oct. 2014.
6. Prasad, A. K. and S. Roy, "Global sensitivity based dimension reduction for fast variability analysis of nonlinear circuits," *2015 IEEE 24th Electrical Performance of Electronic Packaging and Systems (EPEPS)*, 97–100, Oct. 2015.
7. Zhang, Z., T. A. El-Moselhy, I. M. Elfadel, and L. Daniel, "Calculation of generalized polynomialchaos basis functions and gauss quadrature rules in hierarchical uncertainty quantification," *IEEE Transactions on Computer-Aided Design of Integrated Circuits and Systems*, Vol. 33, No. 5, 728–740, May 2014.
8. Zhang, Z., T. W. Weng, and L. Daniel, "Big-data tensor recovery for high-dimensional uncertainty quantification of process variations," *IEEE Transactions on Components, Packaging and Manufacturing Technology*, Vol. 7, No. 5, 687–697, May 2017.
9. Prasad, A. K. and S. Roy, "Accurate reduced dimensional polynomial chaos for efficient uncertainty quantification of microwave/RF networks," *IEEE Transactions on Microwave Theory and Techniques*, Vol. 65, No. 10, 3697–3708, 2017.
10. Blatman, G. and B. Sudret, "Adaptive sparse polynomial chaos expansion based on least angle regression," *Journal of Computational Physics*, Vol. 230, No. 6, 2345–2367, 2011.
11. Larbi, M., I. S. Stievano, F. G. Canavero, and P. Besnier, "Variability impact of many design parameters: The case of a realistic electronic link," *IEEE Transactions on Electromagnetic Compatibility*, Vol. 60, No. 1, 34–41, Feb. 2018.
12. Soize, C. and R. Ghanem, "Physical systems with random uncertainties: Chaos representations with arbitrary probability measure," *SIAM Journal on Scientific Computing*, Vol. 26, No. 2, 395–410, 2004.
13. Berveiller, M., B. Sudret, and M. Lemaire, "Stochastic finite element: A non intrusive approach by regression," *European Journal of Computational Mechanics*, Vol. 15, No. 1-3, 81–92, 2006.
14. Montgomery, D. C., *Design and Analysis of Experiments*, John Wiley & Sons, New York, 2004.
15. Efron, B., T. Hastie, I. Johnstone, and R. Tibshirani, "Least angle regression," *The Annals of Statistics*, Vol. 32, No. 2, 407–499, 2004.
16. Sobol, I. M., "Sensitivity estimates for nonlinear mathematical models," *Mathematical Modelling and Computational Experiments*, Vol. 1, No. 4, 407–414, 1993.

17. Sudret, B., "Global sensitivity analysis using polynomial chaos expansions," *Reliability Engineering & System Safety*, Vol. 93, No. 7, 964–979, 2008.
18. Tang, T. K. and M. S. Nakhla, "Analysis of high-speed VLSI interconnects using the asymptotic waveform evaluation technique," *IEEE Transactions on Computer-Aided Design of Integrated Circuits and Systems*, Vol. 11, No. 3, 341–352, Mar. 1992.
19. Marelli, S. and B. Sudret, "UQLab: A framework for uncertainty quantification in matlab," *Proc. 2nd Int. Conf. on Vulnerability Risk Analysis and Management*, 2554–2563, Liverpool, 2014.
20. McKay, M. D., R. J. Beckman, and W. J. Conover, "A comparison of three methods for selecting values of input variables in the analysis of output from a computer code," *Technometrics*, Vol. 42, No. 1, 55–61, 2000.